ACADEMIC PRESS

Available online at www.sciencedirect.com

SCIENCE DIRECT®

Journal of Sound and Vibration 269 (2004) 183–195

JOURNAL OF SOUND AND VIBRATION

www.elsevier.com/locate/jsvi

Impulsive dynamics of a flexible arm: analytical and numerical solutions

József Kövecses[a,*], William L. Cleghorn[b]

[a] *John H. Chapman Space Centre, Canadian Space Agency, 6767 route de l'Aéroport, St-Hubert, Que., Canada J3Y 8Y9*
[b] *Department of Mechanical and Industrial Engineering, University of Toronto, 5 King's College Rd., Toronto, Ont., Canada, M5S 3G8*

Received 8 October 2001; accepted 15 December 2002

Abstract

Impulsive motion of a flexible, beam-like arm is investigated in this paper. The arm is attached to an inertial system through a revolute joint. A modelling approach and an analytical solution are outlined for this problem. Comparisons are presented between analytical and numerical solutions. Finite motion due to an impulsive event is also considered by simulations, and the results are compared to experimental data.

1. Introduction

The behavior and control of a single flexible arm with a revolute joint has been the subject of extensive research in recent years. This is a relatively simple system that possesses many important hallmarks of more complex flexible systems. Especially the finite motion of single arms has been studied intensively. Finite motion, however, can be greatly influenced by events whose duration is negligible on the time scale determined by the fundamental frequencies of the system. The effects of such events can be described as impulsive motion of the system, where the configuration of the system may be considered unchanged during the time domain of this impulsive motion, and only the velocities change suddenly. The importance of understanding the impulsive motion of a flexible arm, which can lead to the better understanding of the behavior of more complex systems, has of course also been realized, and several research projects have been dedicated to it.

There can be several types of events initiating impulsive motion. Perhaps, the most widely known example is the collision between the end of the beam and an environment (an external

*Corresponding author.
E-mail addresses: jozsef.kovecses@space.gc.ca (J. Kövecses), cleghrn@mie.utoronto.ca (W.L. Cleghorn).

0022-460X/03/$ - see front matter
doi:10.1016/S0022-460X(03)00068-3

object). This is the impulsive event that received the greatest attention (e.g., Refs. [1,2]). Another example having more features of an intelligent, controlled system is the capture of an object by the flexible arm. This example may also be used to represent co-operation between elements of an integrated system. The study of the event of capture has received considerable attention in recent years [3,4].

The description of impulsive motion phenomena was mostly based on Newton's impact law using discretized (finite element or assumed modes) flexible link models. No treatments have been presented for the analytical solution of the impulsive motion problem where a continuous, distributed parameter, flexible beam model is used. In this paper, we present such an analysis. We use the concept of impulsive constraints to treat the impulsive motion as a constrained motion problem. This concept is relatively new in applications related to flexible mechanical systems. Only a few, recent publications considered this powerful approach in solving dynamics and control problems in mechanical systems in connection with robotic applications (e.g., Ref. [5]). We will pay attention only to impulsive motion initiated by either a collision or a capture. We will also give a comparison between analytical results and numerical results obtained by using finite element modelling. In the analysis of the constrained motion model and in the derivation, Jourdain's principle will be used, which besides the d'Alembert–Lagrange principle and Gauss' principle constitutes the third fundamental representation for constrained system dynamics.

The objectives of this work can be summarized as:

- The description of a novel technique will be presented to model the impulsive motion of a flexible beam capable of large rigid body motions. The flexible beam can be considered either using a continuous or a discretized model. We will pay special attention to the continuous model. A general analytical solution will be derived for the impulsive motion of the continuous beam model to determine the discontinuities in the system variables due to an impulsive event at the end of the beam.
- The analytical results will be compared to the results obtained through finite element discretization of the beam for a specific impact configuration. For this configuration, published experimental results are also available for the post-impact finite motion of a slewing flexible beam. These results will be compared to the post-impact motion simulations obtained using the finite element model to assess the analytical and simulation results, and also to investigate the effects of other conditions (e.g., friction) on the impulsive and finite motions of the system.

2. Model for the flexible arm and the object

Consider the system shown in Fig. 1. The arm and the object move in a horizontal plane. It will be assumed that the moment of inertia of the object is negligible, thus only its mass (m_{ob}) enters the formulation. The arm includes a flexible link, an end effector modelled as a rigid body (m_e) at end of the link with negligible moments of inertia, a rigid rotor and a rigid joint (not shown in Fig. 1 in detail). Co-ordinate system $x_0y_0z_0$ is an inertial frame, its unit vectors are $\vec{e}_{x_0}$, $\vec{e}_{y_0}$, $\vec{e}_{z_0}$. Co-ordinate system xyz is a rotating frame attached to the undeformed state[1] of the link or to the rotor, its unit vectors are $\vec{e}_x$, $\vec{e}_y$, $\vec{e}_z$. The flexible link is modelled as a beam. Only its flexural

[1] Undeformed, or rigid body, state means the configuration of the flexible body with no strains and, thus, no stresses.

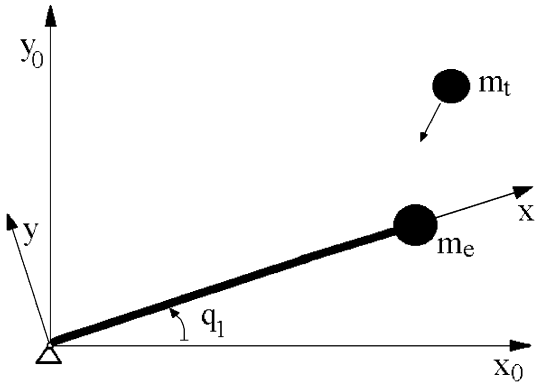

Fig. 1. Flexible link and a moving object.

flexibility is considered. The total mass of the link is m_l and its length is l. The configuration of the system can be completely described by the following co-ordinates. Co-ordinate $q_1(t)$ describes the position of the rotor and thus the position of the rigid body state of the link with respect to the inertial frame; co-ordinates $q_2(t)$ and $q_3(t)$ describe the position of the object. $w(x,t)$ describes the flexural deflections of the link with respect to its rigid body state. The remaining four co-ordinates are the boundary values for the flexible link, $q_4(t)$ gives the flexural displacement of the link at $x=0$, $q_5(t)$ is the rotation of the cross-section of the link at $x=0$, $q_6(t)$ is the flexural displacement of the link at $x=l$, and $q_7(t)$ is the rotation of the cross-section of the link at $x=l$ ("boundary co-ordinates"). Co-ordinates q_i, $(i=1,\ldots,7)$ are time-dependent variables, while $w(x,t)$ is time- and space-dependent variable representing the distributed mass and flexibility of the link. With respect to the rotating frame, the flexible link can be considered as a beam clamped at $x=0$, leading to $q_4=0$ and $q_5=0$. The following summarizes the kinematic quantities necessary to describe the motion of every mass element of the system. The position and velocity of an element of the flexible link with respect to the inertial system may be written as

$$\vec{r}_x = x\vec{e}_x + w\vec{e}_y, \tag{1}$$

and

$$\dot{\vec{r}}_x = -\dot{q}_1 w\vec{e}_x + (x\dot{q}_1 + \dot{w})\vec{e}_y. \tag{2}$$

The position and velocity of the end effector m_e can be obtained as

$$\vec{r}_x = l\vec{e}_x + q_6\vec{e}_y, \tag{3}$$

and

$$\dot{\vec{r}}_e = -\dot{q}_1 q_6\vec{e}_x + (l\dot{q}_1 + \dot{q}_6)\vec{e}_y. \tag{4}$$

The position and velocity of the object are given as

$$\vec{r}_{ob} = q_2\vec{e}_{x_0} + q_3\vec{e}_{y_0}, \tag{5}$$

and

$$\dot{\vec{r}}_{ob} = \dot{q}_2\vec{e}_{x_0} + \dot{q}_3\vec{e}_{y_0}. \tag{6}$$

If the object is an environment incapable of rigid body motion then $\dot{q}_2 = \dot{q}_3 = 0$ has to be used. The position and velocity of an arbitrary element of the rotor are given by $\vec{r}_r$, and $\dot{\vec{r}}_r$, respectively. We do not detail these quantities, because the rotor is modelled as a rigid body rotating about a fixed axis, and thus the resulting expressions can be handled by using known techniques without explicit expression for the kinematic quantities. The system can be considered as a hybrid parameter (discrete and distributed) system since both time-dependent and time- and space-dependent co-ordinates have to be used to represent its configuration.

3. Modelling impulsive motion

Consider that the motion of the system is influenced by an impulsive event (capture or collision) at time t_1 due to the interaction of the end of the arm and the object. The duration of the impulsive event is very short, and on the time scale in use it can be represented by interval $[t_1 - \varepsilon,\ t_1 + \varepsilon,\ \varepsilon \to 0]$. The co-ordinates describing the configuration of the system can be considered unchanged during this interval. Due to the impulsive interaction of the arm and the object, the velocities of the system will change suddenly during this interval. We are interested in determining the ''outcome'' i.e., the post-impact velocities of the system at $t_1 + \varepsilon$. For the post-impact velocities, however, we have certain conditions depending on the initiating impulsive event. For a capture, the post-impact velocity of the end effector and that of the object must be the same. For a collision, one of the impact laws can be used to describe kinetic energy dissipation and to define the coefficient of restitution and the interdependence between the pre- and post-impact states of the system.

These conditions on the post-impact velocities can be represented by impulsive constraints [6–8] for the domain of impulsive motion. For our case, these constraints can be expressed, by using Eqs. (4) and (6), as

$$\dot{q}_2^+ + k_{x_0} = -\dot{q}_1^+ q_6 \cos q_1 - (l\dot{q}_1^+ + \dot{q}_6^+)\sin q_1, \tag{7}$$

and

$$\dot{q}_3^+ + k_{y_0} = -\dot{q}_1^+ q_6 \sin q_1 + (l\dot{q}_1^+ + \dot{q}_6^+)\cos q_1, \tag{8}$$

where $(..)^+$ denotes post-impact velocities, and $(..)^-$ denotes pre-impact velocities. Coefficients k_{x_0} and k_{y_0} need to be determined from the analysis of the impulsive event considered. For example, for a capture situation: $k_{x_0} = k_{y_0} = 0$; for a collision where the relative velocity between the end effector and the object as well as the normal of the impact are parallel to axis y (perpendicular to the arm):

$$k_{x_0} = k_r \sin q_1(-\dot{q}_2^- - \dot{q}_1^- q_6 \cos q_1 - (l\dot{q}_1^- + \dot{q}_6^-)\sin q_1), \tag{9}$$

and

$$k_{y_0} = -k_r \cos q_1(-\dot{q}_3^- - \dot{q}_1^- q_6 \sin q_1 + (l\dot{q}_1^- + \dot{q}_6^-)\cos q_1), \tag{10}$$

where k_r is the coefficient of restitution in the normal direction. (A necessary condition for a collision to occur is that the velocity components must be such that the relative velocity of the object to the end effector be negative.) Other collision situations may require more involved considerations of the contact configuration to determine k_{x_0} and k_{y_0} [9] (e.g., oblique collision with

friction). It has to be mentioned that in the collision case, only single collisions, where contact occurs only one location at a time, can be described properly in this way (like the problem studied here). Multiple, simultaneous collisions may also require the detailed consideration of the sign of each of the transmitted force impulses, which leads to unilateral constraints in the general formulation (as described in Ref. [10]).

In the capture case, the above constraints reduce to the form of inert constraints [8] and continue to exist in the domain of post-impact motion ($t > t_1 + \varepsilon$, finite motion) because the conditions imposed by capture are sustained in that time interval too. For this finite motion, the constraints can be written as

$$\dot{q}_2 = -\dot{q}_1 q_6 \cos q_1 - (l\dot{q}_1 + \dot{q}_6)\sin q_1, \tag{11}$$

and

$$\dot{q}_3 = -\dot{q}_1 q_6 \sin q_1 + (l\dot{q}_1 + \dot{q}_6)\cos q_1. \tag{12}$$

4. Derivation of the analytical solution

We will use Jourdain's principle for the analysis of the system [11,6,12,8]. The impulsive form of this principle for a hybrid parameter system can be expressed as

$$\sum_{i=1}^{n}\left(\frac{\partial T}{\partial \dot{q}_i}\bigg|_{t_1-\varepsilon}^{t_1+\varepsilon} - I_{q_i}\right)\delta_1\dot{q}_i + \int_{(S)}\left(\sum_{z=1}^{p}\left(\frac{\partial K}{\partial \dot{w}_z}\bigg|_{t_1-\varepsilon}^{t_1+\varepsilon} - I_{w_z}\right)\delta_1\dot{w}_z\right) = 0, \tag{13}$$

where $\int_{(S)}(\ldots)$ means summation (integration) over the mass elements of the distributed parameter members of the system, K is the kinetic energy of a mass element of the distributed parameter members, T is the kinetic energy of the system, n is the number of time-dependent coordinates and p is the number of time- and space-dependent variables, I_{q_i} and I_{w_z} are impulses of impressed forces[2] (if any), and $\delta_1\dot{q}_i$ and $\delta_1\dot{w}_z$ are velocity variations. For our case, $n = 7$ and $p = 1$, ($w_1 = w$), K is the kinetic energy of a mass element ($\mathrm{d}m_l = \varrho A\,\mathrm{d}x$) of the flexible link and can be written as

$$K = \tfrac{1}{2}\dot{\vec{r}}_x \cdot \dot{\vec{r}}_x\,\mathrm{d}m_l = \tfrac{1}{2}(\dot{q}_1^2 w^2 + \dot{w}^2 + x^2\dot{q}_1^2 + 2x\dot{q}_1\dot{w})\varrho A\,\mathrm{d}x, \tag{14}$$

and

$$\begin{aligned} T = {} & \frac{1}{2}J_r\dot{q}_1^2 + \frac{1}{2}J_l\dot{q}_1^2 + \frac{1}{2}\varrho A\int_0^l (\dot{q}_1^2 w^2 + \dot{w}^2 + 2x\dot{q}_1\dot{w})\,\mathrm{d}x \\ & + \frac{1}{2}m_{ob}(\dot{q}_2^2 + \dot{q}_3^2) + \frac{1}{2}m_e(\dot{q}_1^2\dot{q}_6^2 + \dot{q}_6^2 + l^2\dot{q}_1^2 + 2l\dot{q}_1\dot{q}_6), \end{aligned} \tag{15}$$

where J_r and J_l are the second moments of inertia of the rotor and the undeformed state of the link about the axis of rotation, m_e and m_{ob} are the masses of the end effector and the object. Velocity variations connect two velocity systems which are both kinematically admissible (satisfy the constraints) at the same time and configuration. The constraint equations yield interdependence conditions for the velocity variations, which give means for further analytical

[2] Impressed forces are also often called applied or given forces in the literature.

considerations. It can be proven [6,8] that velocity variations can be considered continuous quantities in the vicinity of t_1, and must satisfy the post-impact conditions. In our case, from the constraint equations detailed above, the interdependence between the velocity variations in the vicinity of t_1 may be obtained as

$$\delta_1\dot{q}_2 = -\delta_1\dot{q}_1 q_6 \cos q_1 - (l\delta_1\dot{q}_1 + \delta_1\dot{q}_6)\sin q_1, \tag{16}$$

and

$$\delta_1\dot{q}_3 = -\delta_1\dot{q}_1 q_6 \sin q_1 + (l\delta_1\dot{q}_1 + \delta_1\dot{q}_6)\cos q_1. \tag{17}$$

Based on the above equations, and after some derivations, the impulsive form of Jourdain's principle can be expressed for this problem as

$$\begin{aligned}
&\Big[m_e(l^2\dot{q}_1|_-^+ + \dot{q}_6^2\dot{q}_1|_-^+ + l\dot{q}_6|_-^+) + (J_r + J_l)\dot{q}_1|_-^+ \\
&\quad + \int_0^l \varrho A(w^2\dot{q}_1|_-^+ + x\dot{w}|_-^+)\,\mathrm{d}x - I_{q_1}\Big]\delta_1\dot{q}_1 \\
&\quad + \int_0^l [\varrho A(x\dot{q}_1|_-^+ + \dot{w}|_-^+ - I_w)]\delta_1 w\,\mathrm{d}x + [m_e(l\dot{q}_1|_-^+ + \dot{q}_6|_-^+) - I_{q_6}]\delta_1\dot{q}_6 \\
&\quad + [m_{ob}\dot{q}_2|_-^+ - I_{q_2}]\delta_1\dot{q}_2 + [m_{ob}\dot{q}_3|_-^+ - I_{q_3}]\delta_1\dot{q}_3 = 0,
\end{aligned} \tag{18}$$

where $(\ldots)|_-^+ = (\ldots)|_{t_1+\varepsilon} - (\ldots)|_{t_1-\varepsilon}$. In this fundamental equation the velocity variations are not independent of each other due to Eqs. (16) and (17). We will apply a form of the constraint embedding technique (independent velocity variations) [11,6] to further analyze the problem. Based on Eqs. (16) and (17), $\delta_1\dot{q}_1$ and $\delta_1\dot{q}_6$ are selected as independent velocity variations, which is the simplest choice. Using this selection, the fundamental Eq. (18) can be modified as

$$\begin{aligned}
&\Big[m_e(l^2\dot{q}_1|_-^+ + q_6^2\dot{q}_1|_-^+ + l\dot{q}_6|_-^+) + (J_r + J_l)\dot{q}_1|_-^+ \\
&\quad + \int_0^l \varrho A(w^2\dot{q}_1|_-^+ + x\dot{w}|_-^+)\,\mathrm{d}x - m_{ob}(q_6\cos q_1 + l\sin q_1)\dot{q}_2|_-^+ \\
&\quad - m_{ob}(q_6\sin q_1 - l\cos q_1)\dot{q}_3|_-^+ - I_{q_1} + I_{q_2}(q_6\cos q_1 + l\sin q_1) \\
&\quad + I_{q_3}(q_6\sin q_1 - l\cos q_1)\Big]\delta_1\dot{q}_1 + \int_0^l [\varrho A(x\dot{q}_1|_-^+ + \dot{w}|_-^+) - I_w]\delta_1 w\,\mathrm{d}x \\
&\quad + [m_e(l\dot{q}_1|_-^+ + \dot{q}_6|_-^+) - m_{ob}\sin q_1\dot{q}_2|_-^+ + m_{ob}\cos q_1\dot{q}_3|_-^+ - I_{q_6} + I_{q_2}\sin q_1 - I_{q_3}\cos q_1]\delta_1\dot{q}_6 = 0.
\end{aligned} \tag{19}$$

In this equation all velocity variations are independent, thus their coefficients must vanish, and we obtain

$$\begin{aligned}
&m_e(l^2\dot{q}_1|_-^+ + q_6^2\dot{q}_1|_-^+ + l\dot{q}_6|_-^+) + (J_r + J_l)\dot{q}_1|_-^+ + \int_0^l \varrho A(w^2\dot{q}_1|_-^+ + x\dot{w}|_-^+)\,\mathrm{d}x \\
&\quad - m_{ob}(q_6\cos q_1 + l\sin q_1)\dot{q}_2|_-^+ - m_{ob}(q_6\sin q_1 - l\cos q_1)\dot{q}_3|_-^+ \\
&\quad - I_{q_1} + I_{q_2}(q_6\cos q_1 + l\sin q_1) + I_{q_3}(q_6\sin q_1 - l\cos q_1) = 0,
\end{aligned} \tag{20}$$

$$\varrho A(x\dot{q}_1|_-^+ + \dot{w}|_-^+) - I_w = 0, \tag{21}$$

$$m_e(l\dot{q}_1|_-^+ + \dot{q}_6|_-^+) - m_{ob}\sin q_1\dot{q}_2|_-^+ + m_{ob}\cos q_1\dot{q}_3|_-^+ - I_{q_6} + I_{q_2}\sin q_1 - I_{q_3}\cos q_1 = 0. \tag{22}$$

These are the impulsive dynamics equations for the velocities at $t_1+\varepsilon$, which can be solved along with constraint Eqs. (7) and (8). The problem here can be solved in explicit form for the unknown velocities at $t_1+\varepsilon$. The constraints are partially embedded in Eq. (19). To solve the problem explicitly we need to use the constraint equations again. From Eqs. (7) and (8), $\dot{q}_2^+$ and $\dot{q}_3^+$ can be expressed and then, by substituting them, these can be eliminated from the other impulsive dynamics equations. By performing these operations and solving the three impulsive equations, we obtain the velocities which are subjected to sudden impulsive changes ($\dot{q}_1^+,\ \dot{q}_6^+,\ \dot{w}^+$) as

$$\begin{aligned}\dot{q}_1^+ =& \frac{m_e q_6^2 + J_r + \hat{w}^2}{(m_e+m_{ob})q_6^2 + J_r + \hat{w}^2}\dot{q}_1^- - \frac{m_{ob}q_6\cos q_1}{(m_e+m_{ob})q_6^2 + J_r + \hat{w}^2}\left(k_{x_0} + \dot{q}_2^- + \frac{I_{q_2}}{m_{ob}}\right)\\ &- \frac{m_{ob}q_6\sin q_1}{(m_e+m_{ob})q_6^2 + J_r + \hat{w}^2}\left(k_{y_0} + \dot{q}_3^- + \frac{I_{q_3}}{m_{ob}}\right) + \frac{I_{q_1} - lI_{q_6} - \int_0^l xI_w\,\mathrm{d}x}{(m_e+m_{ob})q_6^2 + J_r + \hat{w}^2}\end{aligned} \tag{23}$$

$$\begin{aligned}\dot{q}_6^+ =& \left(\frac{m_e l}{(m_e+m_{ob})} - \frac{(m_e q_6^2 + J_r + \hat{w}^2)l}{(m_e+m_{ob})q_6^2 + J_r + \hat{w}^2}\right)\dot{q}_1^- + \frac{m_e}{m_e+m_{ob}}\dot{q}_6^-\\ &- \left(\frac{m_{ob}\sin q_1}{m_e+m_{ob}} - \frac{m_{ob}q_6 l\cos q_1}{(m_e+m_{ob})q_6^2 + J_r + \hat{w}^2}\right)\left(k_{x_0} + \dot{q}_2^- + \frac{I_{q_2}}{m_{ob}}\right)\\ &- \left(\frac{m_{ob}\cos q_1}{m_e+m_{ob}} - \frac{m_{ob}q_6 l\sin q_1}{(m_e+m_{ob})q_6^2 + J_r + \hat{w}^2}\right)\left(k_{y_0} + \dot{q}_3^- + \frac{I_{q_3}}{m_{ob}}\right)\\ &+ \left(\frac{1}{m_e+m_{ob}} - \frac{l^2}{(m_e+m_{ob})q_6^2 + J_r + \hat{w}^2}\right)I_{q_6}\\ &+ \frac{l}{(m_e+m_{ob})q_6^2 + J_r + \hat{w}^2}\left(I_{q_1} - \int_0^l xI_w\,\mathrm{d}x\right),\end{aligned} \tag{24}$$

and

$$\dot{w}^+ = \dot{w}^- + x(\dot{q}_1^- - \dot{q}_1^+) + \frac{I_w}{\varrho A}, \tag{25}$$

where $\hat{w}^2 = \varrho A\int_0^l w^2\,\mathrm{d}x$. No other velocities are involved in the impulsive motion. This is the general, analytical solution for the impulsive motion of the model of the system. It can be reduced to simpler forms for specific situations, as will be shown later for a particular case. This general solution for the velocity discontinuities can be useful in assessing various discretized modelling approaches for flexible beams experiencing impulsive events, and in designing systems for impact situations. The above results show that the joint ($\dot{q}_1$) and the inner parts of the flexible beam ($\dot{w}$) may also experience a sudden velocity change at $t_1+\varepsilon$. This is because we did not consider the longitudinal flexibility of the beam, and assumed that in the longitudinal direction the beam is "rigid". The fundamental natural frequencies characterizing the longitudinal flexibility of a slender beam are much higher than those pertaining to lateral flexibility. Thus, the dynamic behavior resulting from longitudinal flexibility has a different, "more compressed" time scale than

that of the motion originating from lateral flexibility. Assuming that the beam is "rigid" in the longitudinal direction means that we neglect the time scale of longitudinal flexibility relative to that of lateral flexibility. This may usually be a reasonable assumption that has physical grounds, considering the differences between longitudinal and flexural stiffness values as detailed above. The boundary disturbance occurs in a non-inertial rotating frame, and the rotation of this frame is also a dependent parameter of the problem ($\dot{q}_1^+ \neq \dot{q}_1^-$ generally), because of the elimination of longitudinal flexibility. As a consequence, in general, not only the boundary of the link is subjected to sudden velocity change, but other parts will also experience a sudden velocity change with respect to the inertial frame according to Eq. (25). According to Eq. (23), $\dot{q}_1^+ = \dot{q}_1^-$ can occur only if the deformations of the link vanish at $t_1 - \varepsilon$. It has to be mentioned that this phenomenon is not trivial, and can be pointed out by using continuous flexible body models.

In the following, we consider a special situation where the flexible arm is at rest before the impulsive event with no deformations, $q_1 = 0$, the approaching velocity of the object is perpendicular to the arm, thus $\dot{q}_2^- = 0$, coefficients k_{x_0} and k_{y_0} are equal to zero (capture situation), and no impressed impulsive forces act on the system, $I_{q_1} = 0$, $I_{q_2} = I_{q_3} = I_{q_6} = 0$, $I_w = 0$. For this case, the above general solutions reduce to simpler forms as

$$\dot{q}_1^+ = 0, \quad \dot{q}_6^+ = \dot{w}(l,t)^+ = \frac{m_{ob}}{m_e + m_{ob}} \dot{q}_3^-, \quad \dot{w}^+ = 0. \tag{26}$$

This means that the arm experiences a sudden velocity change only at its tip and the joint will remain at rest immediately after capture. For this case, in the following section, we will present comparisons with finite element solutions concerning the velocity jumps at the tip and at the joint.

5. Numerical solution, simulation and comparison

Discretized models were also developed for the flexible link using finite element modelling based on cubic shape functions. The mathematical model characterizing the impulsive motion of the discretized system can be derived by using impulsive constraints and Jourdain's principle, as was done for the continuous system. The difference is only that the space dependence can now be eliminated by using the cubic shape functions and introducing the corresponding time-dependent co-ordinates to represent the deformation of the link. The analytical results obtained for the continuous system for the post-impact velocities were not used in establishing the finite element solution for the impulsive motion. The first objective was to compare the analytical results and the numerical results obtained using the finite element discretization. We investigated numerically the special case outlined in the previous section with analytical solution given by Eq. (26), where no impressed force impulses (e.g., external disturbances) are present. We have selected the parameters of the flexible arm and the object to be those of an experimental system reported in the literature (Refs. [3,13]). For this experimental system, observations have been reported in Refs. [3,13] regarding the finite motion of the system following the impulsive event (mass capture). (These experimental observations will be used later in this section.) We detail here only the parameters that play a considerable role in the solution of the impulsive motion problem. For the other parameters, which are important in the simulation of the resulted finite motion (estimated joint friction coefficients, etc.), we refer to the cited papers. The parameters of the system are as follows:

Table 1
Finite element solutions for the impulsive motion

Number of elements	$\dot{q}_1^+$ (rad/s)	$\dot{q}_6^+$ (m/s)
5	-0.002694259	-0.356824511
10	-1.34875×10^{-6}	-0.360333552
15	-1.10525×10^{-9}	-0.360856424
20	-1.73×10^{-12}	-0.361117939

beam length, 0.725 m; beam cross-sectional area: $3.175 \times 10^{-4}\,\mathrm{m}^2$, second moment of area of beam: $2.67 \times 10^{-10}\,\mathrm{m}^4$; Young's modulus: 6.5×10^{10} Pa, beam linear mass density, 0.874 kg/m; Hub inertia, $1.3233 \times 10^{-4}\,\mathrm{kg\,m}^2$, end effector mass, 0.55 kg; mass of the object: 0.5 kg, velocity difference between the end effector and the object before capture, -0.76 m/s. For such parameters, the numerical values of the analytical solutions, according to Eq. (26), are $\dot{q}_1^+ = 0$ and $\dot{q}_6^+ = -0.361904762$ m/s. The finite element solutions obtained employing various numbers of elements are shown in Table 1. As the number of finite elements is increased, the numerical solutions converge to the analytical solutions. This means that the finite element model of the link can be used with confidence in predicting the impulsive motion of the arm caused by the impulsive event of dynamic mass capture. By employing 15–20 finite elements, the impulsive motion can be predicted very accurately.

Our next objective was to investigate the post-impact finite motion of the arm (this motion is the result of the impulsive event), and compare the results with that of the experimental investigation. In the experiment, as described in Ref. [13], a rail-guided platform (''rail-car''), upon which the object sits, was used to deliver the object for capture to the end effector with a prescribed velocity. At the time of capture, the platform misses the object and continues to move further (down an incline), while the object attaches to the end effector and starts to move together with it. The details of the experiment can be found in Refs. [3,13]. Experimental observations were reported concerning two main features of the system's finite motion after capture. The first was the time history of the flexible deflection of the tip of the beam in the initial period of 1 s. The second feature was the time history of the joint angle during a period of 10 s following mass capture. We also investigated these two features in the simulation of the finite motion of the system. The detailed equations of motion for the finite motion of the system have also been developed using finite element modelling. The analytical results obtained for the impulsive motion were applied as input initial values to the model describing the finite motion. It has to be noted that the finite element solution obtained for the impulsive motion (Table 1) could have been used here to replace the analytical solution, since it also gives accurate results, as shown in Table 1. A more detailed description on these simulations can be found in Ref. [14]. Ten finite elements were used to approximate link flexibility. Numerical integrations, for finite motion following mass capture, were performed by using fifth and eighth order explicit Runge–Kutta methods (Dormand and Prince algorithms, see details in Refs. [15,16]).

In the simulation of motion of a mechanical system, one of the most difficult problems is to accurately account for static friction and stick-slip motion in the joints. To consider these phenomena, we have used the so-called ''equivalent force method'' which was proposed in Ref. [17] and extended further in Ref. [18]. This type of treatment is useful when there are only a few

"simultaneous" frictional interfaces, and can basically be considered as a special case of the general method described in Ref. [10].

An interesting phenomenon due to friction is the influence of the detachment transition on the impulsive and post-impact motions of the system. This transition happens at the time of capture when static friction forces between the rail-car and the object must be overcome to detach the object from the rail-car, and at least for a very short period of time the object will slide on the rail-car before separation. This phenomenon was first left unmodelled in the analytical solution for impulsive motion and also during the numerical simulations, which resulted in differences in magnitude between the simulated and experimentally observed tip deflection response of the beam. To consider these effects, it has to be realized that the resultant interaction force between the rail-car and the object can be impulsive due to the discontinuous change in the system topology Ref. [14]. This force has to be considered as an external, impressed force impulse in the impulsive motion formulation, as given in the general solution, Eqs. (23)–(25), to model the effects of detachment. The simplified solution given for this problem in Eq. (26) does not account for the force impulse. Thus, we need to modify the simplified solution for the impulsive motion based on Eqs. (23)–(25). The force impulse due to the detachment transition will act in the direction the object is forcing the arm to move. This direction is perpendicular to the arm for this particular setup (as was discussed earlier), hence, I_{q_3} describes its effects in Eqs. (23)–(25). The simplified solution for this case can then be obtained from these equations as

$$\dot{q}_1^+ = 0, \;\; \dot{q}_6^+ = \dot{w}(l,t)^+ = \frac{m_{ob}}{m_e + m_{ob}}\left(\dot{q}_3^- + \frac{I_{q_3}}{m_{ob}}\right), \;\; \dot{w}^+ = 0. \tag{27}$$

For the experimental setup there were no parameters available for the friction interaction between the rail-car and the object to estimate I_{q_3}. A relatively small static friction coefficient with a magnitude of 0.05 was assumed and a Dirac delta type force function was used to model I_{q_3} to obtain the solution for the impulsive motion based on Eq. (27). The simulation results obtained considering these effects gave a tip deviation response, the magnitude of which is very close to the experimentally observed response.

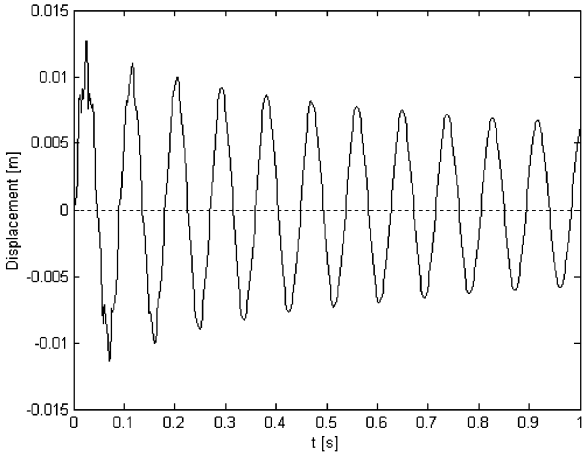

Fig. 2. Computed tip deflection response of the flexible link.

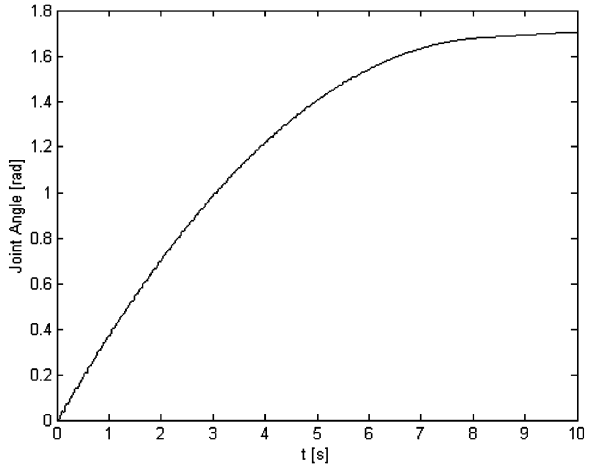

Fig. 3. Computed joint angle response of the arm.

For the flexible defection of the tip of the beam in the first second of motion, our results are shown in Fig. 2, considering 500 samples per second. In the frequency and phase of motion, and in the magnitudes of the deflections there is good agreement between the experimental data (Refs. [3,13]) and our computed results.

For the time history of the joint angle during a period of 10 s, our computational results are shown in Fig. 3 using 50 samples/s. Considering that the joint friction parameters are only estimated values, these results are in good agreement with the experimental observations. By performing several simulations, we found that in the initial phase of motion, the dynamic friction is more dominant than the static friction in influencing the nature of motion. However, later, static friction becomes prevalent.

We also evaluated the influence of two damping terms, Rayleigh damping and friction, on the finite motion of the system by several simulations, considering models with and without these terms. It was found that friction is the primary, dominant means for energy loss during finite motion. The presence or lack of Rayleigh damping in this example only very slightly influences the behavior of the system.

Simulations for the post-impact finite motion of the system employing various numbers of finite elements were also performed. It was found that to represent the overall behavior of the system including both impulsive motion and finite motion, the use of 5–10 finite elements is sufficient to achieve reasonable accuracy. This is in agreement with the results obtained by considering the pure impulsive motion only, as presented in Table 1. Further increasing the number of elements did not result in significant increase in accuracy, but it caused significantly greater times in computations. This observation is also supported by Ref. [19], where various contact models were considered for beams for use in vehicle crash-worthiness analysis.

6. Conclusions

In this paper the impulsive motion of a one-link flexible arm has been investigated. Impulsive events due to capture of an object or collision with an object have been studied. The flexible link

was considered as a continuous beam. An analytical solution has been outlined for the problem using the theory of hybrid parameter mechanical systems and modelling impulsive events as constrained motion problems. According to our knowledge, this general solution has not been presented before. This solution for the velocity discontinuities can be useful to assess various modelling approaches for flexible beams experiencing impulsive events as well as to assist in design processes involving impact situations. As discussed in Section 4, it can also be used to point out non-trivial phenomena occurring in flexible systems due to impulsive events. A comparison has been carried out and presented between the analytical solution and numerical, finite element solutions. By increasing the number of elements in the discretized model, the numerical solutions converge to the analytical results. A relatively small number of elements (5–10 elements) may be sufficient to represent the behavior of the system with reasonable accuracy. Finite motion resulted from an impulsive event was also studied by simulations, and the results were compared to experimental data. Good agreement has been found between the two sets of data. It was also noticed that frictional interfaces have substantial effect on both impulsive and finite motions of the experimental system.

This paper was mainly concerned with the analysis of a single rotating flexible beam. However, the main framework of the work can be extended and applied for more complex systems as well. The technique to model impulsive events using impulsive constraints, and the method to derive analytical solutions for impulsive motion are generally valid [6]. It will be a future goal to derive analytical solutions for multibody systems consisting of flexible beams to study various impact situations and make assessments using experimental data.

References

[1] B.V. Chapnik, G.R. Heppler, J.D. Aplevich, Modeling impact on a one-link flexible robotic arm, IEEE Transactions on Robotics and Automation 7 (1991) 479–488.
[2] A.S. Yigit, A.G. Ulsoy, R.A. Scott, Dynamics of a radially rotating beam with impact Part 1 and Part 2, American Society of Mechanical Engineers Journal of Vibration and Acoustics 112 (1990) 65–77.
[3] G.R. Heppler, On the dynamic mass capture by flexible robots, in: A.K. Morris (Ed.), Control of Flexible Structures, American Mathematical Society, Providence, RI, 1993, pp. 157–177.
[4] K.H. Hwang, A.A. Shabana, Effect of mass capture on the propagation of transverse waves in rotating beams, Journal of Sound and Vibration 186 (1995) 495–525.
[5] N. Sarkar, X. Yun, R. Ellis, Live-constraint-based control for contact transitions, IEEE Transactions on Robotics and Automation 14 (1998) 743–754.
[6] J. Kövecses, W.L. Cleghorn, Finite and impulsive motion of constrained mechanical systems via Jourdain's principle: discrete and hybrid parameter models, International Journal of Non-Linear Mechanics 38 (2003) 935–956.
[7] J.G. Papastavridis, Impulsive motion of ideally constrained mechanical systems via analytical dynamics, International Journal of Engineering Science 27 (1989) 1445–1461.
[8] L.A. Pars, A Treatise on Analytical Dynamics, Heinemann, London, 1965.
[9] W.J. Stronge, Impact Mechanics, Cambridge University Press, Cambridge, 2000.
[10] F. Pfeiffer, C. Glocker, Multibody Dynamics with Unilateral Contacts, Wiley, New York, 1996.
[11] L.Y. Bahar, On the use of quasi-velocities in impulsive motion, International Journal of Engineering Science 32 (1994) 1669–1686.
[12] J.G. Papastavridis, On Jourdain's principle, International Journal of Engineering Science 30 (1992) 135–140.

[13] B.J. Rhody, G.R. Heppler, M.F. Golnaraghi, Dynamic mass capture by a single flexible link, in: C.L. Kirk, P.C. Hughes (Eds.), Dynamics and Control of Structures in Space II, Computational Mechanics Publication, Southampton, 1993, pp. 109–124.
[14] J. Kövecses, W.L. Cleghorn, R.G. Fenton, Dynamic modeling and analysis of a robot manipulator intercepting and capturing a moving object with the consideration of structural flexibility, Multibody System Dynamics 3 (1999) 137–162.
[15] E. Hairer, S.P. Norsett, G. Wanner, Solving Ordinary Differential Equations I: Nonstiff Problems, 2nd Edition, Springer, Berlin, 1993.
[16] E. Hairer, G. Wanner, Solving Ordinary Differential Equations II: Stiff and Differential-Algebraic Problems, Springer, Berlin, 1991.
[17] D. Karnopp, Computer simulation of stick–slip friction in mechanical dynamic systems, American Society of Mechanical Engineers Journal of Dynamic Systems Measurement and Control 107 (1985) 100–103.
[18] A.A. Ferri, B.S. Heck, Analysis of stick-slip motion in Coulomb damped systems using variable structure system theory, Proceedings of the ASME Design Engineering Technical Conferences, 16th Biennial Conference on Mechanical Vibration and Noise, Sacramento, CA, Paper # DETC97/VIB-3915, 1997.
[19] J.A.C. Ambrósio, Impact of rigid and flexible multibody systems: deformation description and contact models, in: W. Schiehlen, M. Valášek (Eds.), Virtual Nonlinear Multibody Systems, NATO Science Series: II, Vol. 103, Kluwer, Dordrecht, 2003, pp. 15–33.